LETTERS

c-Myc suppression of miR-23a/b enhances mitochondrial glutaminase expression and glutamine metabolism

Ping Gao[1], Irina Tchernyshyov[2], Tsung-Cheng Chang[3], Yun-Sil Lee[3], Kayoko Kita[11], Takafumi Ochi[11], Karen I. Zeller[1], Angelo M. De Marzo[6,7,8], Jennifer E. Van Eyk[2,9], Joshua T. Mendell[3,4,5] & Chi V. Dang[1,3,5,6,7,10]

Altered glucose metabolism in cancer cells is termed the Warburg effect, which describes the propensity of most cancer cells to take up glucose avidly and convert it primarily to lactate, despite available oxygen[1,2]. Notwithstanding the renewed interest in the Warburg effect, cancer cells also depend on continued mitochondrial function for metabolism, specifically glutaminolysis that catabolizes glutamine to generate ATP and lactate[3]. Glutamine, which is highly transported into proliferating cells[4,5], is a major source of energy and nitrogen for biosynthesis, and a carbon substrate for anabolic processes in cancer cells, but the regulation of glutamine metabolism is not well understood[1,6]. Here we report that the c-Myc (hereafter referred to as Myc) oncogenic transcription factor, which is known to regulate microRNAs[7,8] and stimulate cell proliferation[9], transcriptionally represses miR-23a and miR-23b, resulting in greater expression of their target protein, mitochondrial glutaminase, in human P-493 B lymphoma cells and PC3 prostate cancer cells. This leads to upregulation of glutamine catabolism[10]. Glutaminase converts glutamine to glutamate, which is further catabolized through the tricarboxylic acid cycle for the production of ATP or serves as substrate for glutathione synthesis[11]. The unique means by which Myc regulates glutaminase uncovers a previously unsuspected link between Myc regulation of miRNAs, glutamine metabolism, and energy and reactive oxygen species homeostasis.

Oncogenes and tumour suppressors have been linked to the regulation of glucose metabolism, thereby connecting genetic alterations in cancers to their glucose metabolic phenotype[1,2]. In particular, the *MYC* oncogene produces Myc protein that directly regulates glucose metabolic enzymes as well as genes involved in mitochondrial biogenesis[9,12]. In this regard, we sought to determine the role of *MYC* in altering the mitochondrial proteome in order to understand further the regulation of tumour metabolism. We studied human P-493 B cells that bear a tetracycline-repressible *MYC* construct, such that tetracycline withdrawal results in rapid induction of Myc and mitochondrial biogenesis, followed by cell proliferation[12,13]. By comparing the mitochondrial proteomes of tetracycline-treated and untreated cells with high Myc expression, we found eight mitochondrial proteins that are distinctly differentially expressed in response to Myc (Fig. 1a, b and Supplementary Table 1). Mitochondrial glutaminase expression (GLS, molecular mass of ~58 kDa) was increased ~10-fold in response to Myc. As such, we determined the response of glutaminase to Myc induction in a time-course study using anti-GLS antibody[10] (Fig. 1c) and found that GLS levels diminish with decreased Myc expression and recover on Myc re-induction. However, the level of the mitochondrial protein TFAM remained virtually unaltered. GLS levels also correlate with Myc levels in another human B cell line (CB33) and one (CB33-Myc) with constitutive Myc expression[14]. Because human prostate cancer is linked to Myc expression[15], we sought to determine whether reduction of Myc expression by short interfering RNA (siRNA) in the human PC3 prostate cancer cell line is also associated with reduction of GLS expression (Fig. 1d). Similar to the human lymphoid cells, the PC3 cells also displayed a correlation between Myc and GLS levels.

We then sought to determine whether the marked alteration of GLS levels in response to Myc is functionally linked to Myc-induced cell proliferation. Although there are two major known tissue-specific GLS isoforms, GLS1 and GLS2 (refs 16, 17), our data show that only GLS1 is predominantly expressed in P493-6 or PC3 cells (Supplementary Fig. 1). We first determined whether gain of GLS1 function through overexpression in PC3 cells would rescue the diminished growth rate associated with siRNA-mediated reduction of Myc (Supplementary Fig. 2) and found that ectopic GLS1 expression alone is insufficient to stimulate growth. In light of the observation that no single gene could substitute for Myc[18,19] and that Myc is a pleiotropic transcription factor[9], this outcome was not particularly surprising. As such, we reduced the expression of GLS1 (hereafter referred to as GLS) by RNA interference (*GLS* siRNA) and found that P-493-6 cell proliferation is markedly attenuated by *GLS* siRNA but not by control siRNA (Fig. 2a). Likewise, proliferation of the human PC3 prostate cancer cell line was diminished by *GLS* siRNA (Fig. 2a), indicating that GLS is necessary for cell proliferation.

Because glutamine is converted by GLS to glutamate for further catabolism by the tricarboxylic acid (TCA) cycle, and previous studies indicate that overexpression of Myc sensitizes human cells to glutamine-withdrawal-induced apoptosis[11], we determined the metabolic responses of P493-6 or PC3 cells to glutamine deprivation (Fig. 2b). The growth of both cell lines was diminished significantly by glutamine withdrawal and moderately with glucose withdrawal. Glutamine withdrawal also resulted in a decrease in ATP levels (Fig. 2c) associated with a diminished cellular oxygen consumption rate (Supplementary Fig. 3a, b). Reduction of GLS by RNA interference (RNAi) also reduced ATP levels (Fig. 2d). Because glutamine is a precursor for glutathione[20], glutathione levels were measured by flow cytometry and were found to be diminished with glutamine withdrawal or RNAi-mediated reduction of GLS (Supplementary Fig. 4 and Supplementary Table 2) that is also associated with an increase in reactive oxygen species (ROS) levels (Supplementary Fig. 3c) and cell death in the P493-6 cells (Fig. 2e and Supplementary Fig. 5). Of note,

[1]Division of Hematology, Department of Medicine, [2]Division of Cardiology, Department of Medicine, [3]McKusick-Nathans Institute of Genetic Medicine, [4]Departments of Pediatrics and [5]Molecular Biology and Genetics, [6]Departments of Pathology, [7]Oncology, [8]Urology, [9]Biological Chemistry and [10]Cell Biology, Johns Hopkins University School of Medicine, Baltimore, Maryland 21205, USA. [11]Laboratory of Toxicology, Faculty of Pharmaceutical Sciences, Teikyo University, Sagamiko, Kanagawa 229-0195, Japan.

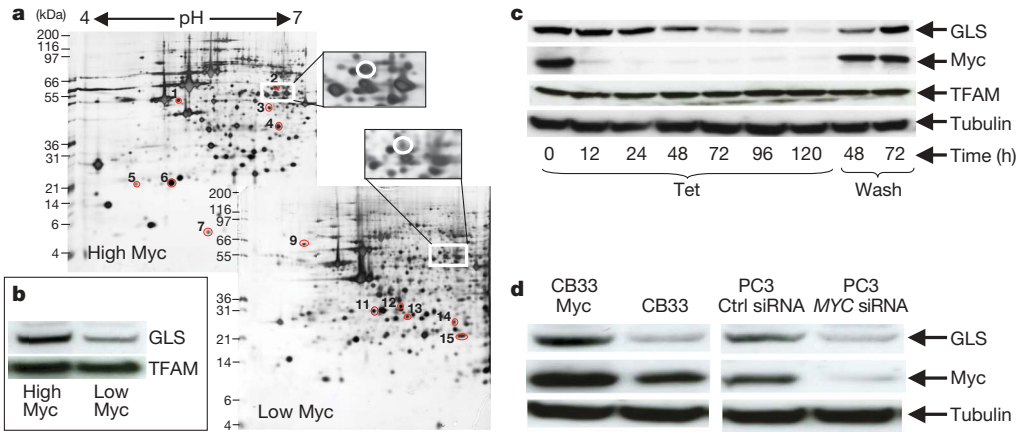

Figure 1 | Myc enhances the expression of mitochondrial protein glutaminase. **a**, The expanded insets of two-dimensional gels reveal the induction of glutaminase (GLS; highlighted by white circles) by Myc in P493-6 B cells. For each condition, 350 μg of mitochondrial protein lysate was resolved on 18 cm immobilized pH gradient strips as the first dimension followed by 10% Bis-Tris SDS–PAGE as the second dimension, which is marked by molecular mass markers. Protein spots were visualized by silver staining. Six independent biological experiments were performed for each condition. Supplementary Table 1 summarizes the identity of the spots with the same numbering system as depicted in the figure. **b**, Immunoblot with anti-GLS antibody of a one-dimensional SDS–PAGE gel of mitochondrial proteins (20 μg per lane) validates the induction of GLS by Myc discovered in **a**. TFAM represents a control mitochondrial protein. **c**, P493-6 cells were treated with tetracycline (Tet) for different lengths of time to inhibit Myc expression or were treated first with tetracycline for 48 h and then washed (Wash) to remove tetracycline, with the times after wash-out indicated. Cells were then harvested for immunoblot assay for GLS or c-Myc. Anti-tubulin antibody and anti-TFAM were used for loading controls. **d**, Human CB33 lymphoblastoid cells, CB33-Myc cells and PC3 cells transfected with siRNA against c-Myc (*MYC* siRNA) or control siRNA (Ctrl siRNA) were used for immunoblot assays. Experiments were replicated with similar results.

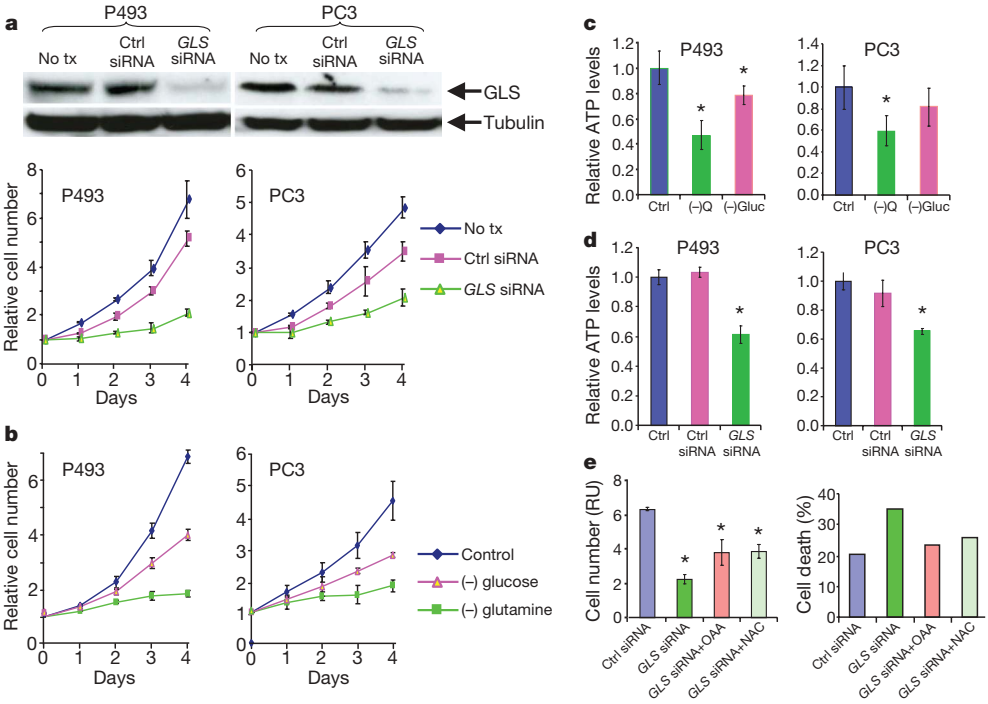

Figure 2 | Glutamine and glutaminase are necessary for Myc-mediated cancer cell proliferation and survival. **a**, Top: immunoblots showing that GLS protein level is diminished by transfecting cells with siRNA for *GLS1* (*GLS* siRNA) as compared with non transfection (No tx) or control siRNA (Ctrl siRNA). Bottom: growth inhibition of P493 and PC3 cells by *GLS* siRNA. The results shown are mean ± s.d., $n = 3$. **b**, Growth inhibition of P493 and PC3 cells cultured under control, glucose- or glutamine-deprived conditions. The results shown are mean ± s.d., $n = 3$. **c**, Cells were cultured with normal medium or medium without glucose ((−)Gluc)or glutamine ((−)Q) for 48 h and harvested for ATP assay as described in Methods. The results shown (mean ± s.d., $n = 2$) are relative ATP levels per microgram total protein normalized to the control (Ctrl) normal medium group. **d**, ATP levels in control cells or cells transfected with *GLS* siRNA or control siRNA. Seventy-two hours after transfection, cells were harvested for ATP assay. The results shown (mean ± s.d., $n = 2$) are relative ATP levels per microgram total protein normalized to the non-transfected control group. **e**, Cells were transfected with *GLS* siRNA or control siRNA and cultured with 10 mM *N*-acetylcysteine (NAC), or 5 mM oxaloacetate (OAA), as indicated. The left panel shows cell counts (relative units (RU); mean ± s.d., $n = 5$) of different groups at 72 h after transfection (see Supplementary Fig. 5 for the complete cell growth curve). The right panel shows the percentage cell death at 72 h after transfection. Percentage cell death indicates annexin-positive plus annexin V and 7-AAD-positive cells. Primary data are shown in Supplementary Fig. 4. All experiments in Fig. 2 were repeated at least twice. All experiments with P493 cells were in the absence of tetracycline. Asterisk denotes mean (±s.d.) that is significantly different from control ($P < 0.05$, *t* test).

shortly after the *MYC* proto-oncogene was discovered, the MC29 retrovirus which bears the v-*myc* oncogene was found to enhance glutamine catabolism and mitochondrial respiration in transplantable avian liver tumour cells[21]. Thus, our findings functionally link historical observations with Myc, glutaminase and glutamine metabolism.

Because GLS catabolizes glutamine for ATP and glutathione synthesis, its reduction affects proliferation and cell death presumably through depletion of ATP and augmentation of ROS, respectively. Hence, we sought to rescue the P493-6 cells with the TCA cycle metabolite oxaloacetate (OAA) and the oxygen radical scavenger *N*-acetylcysteine (NAC)[11]. Both OAA and NAC partially rescued the decreased proliferation and death of P493-6 cells deprived of GLS (Fig. 2e and Supplementary Fig. 6). Similarly, OAA and NAC both partially rescued glutamine-deprived P493-6 cells (Supplementary Figs 5 and 6). These findings support the notion that glutamine catabolism through GLS is critical for cell proliferation induced by Myc and protection against ROS generated by enhanced mitochondrial function in response to Myc[11,20].

Given that GLS is critical for cell proliferation and is induced by Myc, we determined the mechanism by which Myc regulates GLS. Because Myc is a transcription factor[9], we hypothesized that Myc transactivates GLS directly as a target gene. Despite the presence of a canonical Myc binding site (5′-CACGTG-3′) in the *GLS* gene intron 1, *GLS* messenger RNA levels do not respond to alterations in Myc levels in the P493-6 cells, suggesting that GLS is regulated at the post-transcriptional level (Fig. 3a). As such, we hypothesized that GLS could be regulated by miRNAs that are in turn directly regulated by Myc. The TargetScan algorithm predicts that miR-23a and miR-23b could target the GLS 3′ untranslated region (UTR) seed sequence. Notably, our earlier studies uncovered that both miR-23a and miR-23b are suppressed by Myc in P493-6 cells[7], and both miR-23a and miR-23b are decreased in human prostate cancers[22], which are associated with elevated Myc expression[15].

To verify that miR-23a and miR-23b (hereafter referred to as miR-23a/b) are suppressed by Myc and can be diminished by antisense miR-23a/b locked nucleic acid (LNA) oligomers, a northern blot analysis was performed; the results show that miR-23a/b are indeed suppressed by Myc and profoundly diminished by antisense miR-23a/b LNAs (Fig. 3b). Quantitative real-time polymerase chain reaction (PCR) assays show (Supplementary Fig. 7) that miR-23a/b levels increase with diminished Myc expression and then decrease on Myc re-induction in a manner that is compatible with the GLS protein levels seen in Fig. 1c. We also found an inverse relationship between Myc and the levels of miR-23a/b in the CB33 human lymphoid cells and PC3 prostate cancer cell line (Supplementary Fig. 8). Furthermore, a chromatin immunoprecipitation assay (Fig. 3c) shows that Myc directly binds the transcriptional unit, *C9orf3*, encompassing miR-23b, as demonstrated for other Myc miRNA targets[7]. Because the transcriptional unit involving miR-23a has not been mapped, we did not study miR-23a in this context. These observations indicate that Myc represses miR-23a and miR-23b, which seem to be directly regulated by Myc.

We next determined whether miR-23a/b target and inhibit the expression of GLS through the 3′ UTR. In this regard, we cloned the 3′ UTR sequence of *GLS* including the predicted binding site for miR-23a/b to the pGL3 luciferase reporter vector and transfected MCF-7 cells, which are known to express miR-23a/b (ref. 23). The *GLS* 3′ UTR inhibited luciferase activity in a fashion that was blocked by co-transfection with the antisense miR-23a/b LNAs, but not with

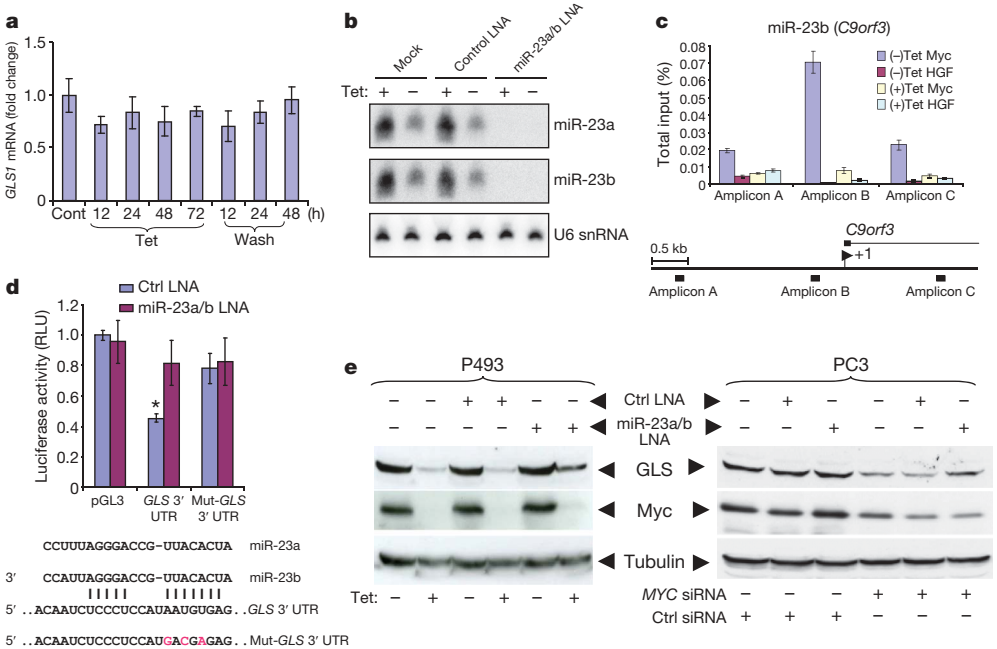

Figure 3 | Myc increases GLS protein by transcriptionally repressing miR-23a/b that target the *GLS* 3′ UTR. a, *GLS1* mRNA levels were determined by real-time PCR after treatment of P493 cells with tetracycline or on removal of tetracycline (after 48 h of tetracycline pre-treatment). Data are mean ± s.d., $n = 3$ PCR reactions. **b**, Northern blot analysis of miR-23a/b expression in P493 cells treated with or without tetracycline for 24 h and then transfected with miR-23a/b LNAs or scrambled control LNA and cultured for 48 h. **c**, Chromatin immunoprecipitation assay with P493 cells showing Myc binding to the promoter region of *C9orf3*, whose transcript is processed to miR-23b. The positions of the amplicons are depicted in the cartoon of the *C9orf3* gene below the bar graphs (mean ± s.d., $n = 3$). Anti-HGF serves as a nonspecific antibody control. **d**, Inhibition of *GLS* 3′ UTR luciferase reporter by miR-23a/b. Top: glutaminase reporter (wild-type *GLS* 3′ UTR or mutant Mut-*GLS* 3′ UTR) or control (pGL3) luciferase constructs were co-transfected with pSV-Renilla into MCF-7 cells, or further co-transfected with miR-23a/b LNAs or control LNA. After 24 h, luciferase activities (relative light units, RLU) were measured. Data shown are RLUs normalized to the control group (mean ± s.d., $n = 4$). Bottom: miR-23a, miR-23b, *GLS* 3′ UTR and Mut-*GLS* 3′ UTR sequences. **e**, Analysis of GLS protein levels in P493 and PC3 cells treated with control or antisense miR-23a/b LNAs. Left: P493 cells were treated with or without tetracycline for 24 h and then transfected with antisense miR-23a/b LNAs or scrambled control LNA. After 72 h, cells were harvested for immunoblot assay. Right: PC3 cells were transfected with *MYC* siRNA or control siRNA. After 24 h, cells were transfected with miR-23a/b LNAs or scrambled control. Cells were cultured for 72 h and then were harvested for immunoblot assay.

control LNAs (Fig. 3d). We next mutated the predicted binding site by a site-directed mutagenesis strategy[8] and observed that mutant 3′ UTR does not inhibit luciferase activity as the wild-type sequence does. Using these reporters in PC3 cells, we observed that diminished expression of Myc via siRNA results in decreased luciferase activity with wild type but not with the mutant 3′ UTR reporter (Supplementary Fig. 9). Notably, reduced GLS protein level, a result of decreased Myc expression (Fig. 1c), was rescued by antisense miR-23a/b LNAs (Fig. 3e). The antisense miR-23a/b LNAs also partially rescued the diminished GLS level associated with RNAi-mediated reduction of Myc expression in PC3 cells (Fig. 3e).

We also examined events upstream and downstream of *GLS*[24] and found that the glutamine transporter SLC7A5 is induced by Myc in P493-6 cells at the transcriptional level (fivefold by nuclear run-on, with a >7-fold induction of its mRNA level (K.I.Z. and C.V.D, unpublished data). The glutamine transporter ASCT2 (also called SLC1A5) shows a twofold induction by Myc at the mRNA level, whereas glutamate dehydrogenase mRNA levels appear unaltered (K.I.Z. and C.V.D., unpublished data). Furthermore, we found that elevated levels of Myc protein in human prostate cancer correspond to levels of GLS, which are not increased in the accompanying normal tissue from the same patients (Supplementary Fig. 10). Intriguingly, miR-23a and miR-23b are significantly decreased in human prostate cancer as compared with normal prostate tissue[22]. It is notable that loss of GLS function by antisense suppression significantly inhibits the tumorigenesis of Ehrlich ascites tumour cells *in vivo*[25]. Our findings uncover a pathway by which Myc suppression of miR-23a/b, which target GLS, enhances glutamine catabolism through increased mitochondrial glutaminase expression. Taken together, these observations provide a regulatory mechanism involving Myc and miRNAs for elevated expression of glutaminase and glutamine metabolism in human cancers.

METHODS SUMMARY

Human cell lines were cultured under standard conditions. Isolation of mitochondria, enrichment for mitochondrial proteins, and proteomic analysis were performed as described[26–29]. RNA interference experiments and luciferase reporter analysis of miRNA activity were as reported[8,30]. Flow cytometric analyses of reactive oxygen species, cell death and glutathione level were performed as described[11,30]. Human samples were acquired with the approval of the Johns Hopkins University School of Medicine Institutional Review Board.

Full Methods and any associated references are available in the online version of the paper at www.nature.com/nature.

Received 20 August 2008; accepted 27 January 2009.
Published online 15 February 2009.

1. Deberardinis, R. J., Sayed, N., Ditsworth, D. & Thompson, C. B. Brick by brick: metabolism and tumor cell growth. *Curr. Opin. Genet. Dev.* **18,** 54–61 (2008).
2. Kroemer, G. & Pouyssegur, J. Tumor cell metabolism: cancer's Achilles' heel. *Cancer Cell* **13,** 472–482 (2008).
3. DeBerardinis, R. J. *et al.* Beyond aerobic glycolysis: transformed cells can engage in glutamine metabolism that exceeds the requirement for protein and nucleotide synthesis. *Proc. Natl Acad. Sci. USA* **104,** 19345–19350 (2007).
4. Reitzer, L. J., Wice, B. M. & Kennell, D. Evidence that glutamine, not sugar, is the major energy source for cultured HeLa cells. *J. Biol. Chem.* **254,** 2669–2676 (1979).
5. Gallagher, F. A., Kettunen, M. I., Day, S. E., Lerche, M. & Brindle, K. M. ^{13}C MR spectroscopy measurements of glutaminase activity in human hepatocellular carcinoma cells using hyperpolarized ^{13}C-labeled glutamine. *Magn. Reson. Med.* **60,** 253–257 (2008).
6. Curthoys, N. P. & Watford, M. Regulation of glutaminase activity and glutamine metabolism. *Annu. Rev. Nutr.* **15,** 133–159 (1995).
7. Chang, T. C. *et al.* Widespread microRNA repression by Myc contributes to tumorigenesis. *Nature Genet.* **40,** 43–50 (2008).
8. O'Donnell, K. A., Wentzel, E. A., Zeller, K. I., Dang, C. V. & Mendell, J. T. c-Myc-regulated microRNAs modulate E2F1 expression. *Nature* **435,** 839–843 (2005).
9. Eilers, M. & Eisenman, R. N. Myc's broad reach. *Genes Dev.* **22,** 2755–2766 (2008).
10. Kita, K., Suzuki, T. & Ochi, T. Down-regulation of glutaminase C in human hepatocarcinoma cell by diphenylarsinic acid, a degradation product of chemical warfare agents. *Toxicol. Appl. Pharmacol.* **220,** 262–270 (2007).
11. Yuneva, M., Zamboni, N., Oefner, P., Sachidanandam, R. & Lazebnik, Y. Deficiency in glutamine but not glucose induces MYC-dependent apoptosis in human cells. *J. Cell Biol.* **178,** 93–105 (2007).
12. Li, F. *et al.* Myc stimulates nuclearly encoded mitochondrial genes and mitochondrial biogenesis. *Mol. Cell. Biol.* **25,** 6225–6234 (2005).
13. Schuhmacher, M. *et al.* Control of cell growth by c-Myc in the absence of cell division. *Curr. Biol.* **9,** 1255–1258 (1999).
14. Lombardi, L., Newcomb, E. W. & Dalla-Favera, R. Pathogenesis of Burkitt lymphoma: expression of an activated c-myc oncogene causes the tumorigenic conversion of EBV-infected human B lymphoblasts. *Cell* **49,** 161–170 (1987).
15. Gurel, B. *et al.* Nuclear MYC protein overexpression is an early alteration in human prostate carcinogenesis. *Mod. Pathol.* **21,** 1156–1167 (2008).
16. Perez-Gomez, C. *et al.* Co-expression of glutaminase K and L isoenzymes in human tumour cells. *Biochem. J.* **386,** 535–542 (2005).
17. Turner, A. & McGivan, J. D. Glutaminase isoform expression in cell lines derived from human colorectal adenomas and carcinomas. *Biochem. J.* **370,** 403–408 (2003).
18. Berns, K., Hijmans, E. M., Koh, E., Daley, G. Q. & Bernards, R. A genetic screen to identify genes that rescue the slow growth phenotype of c-myc null fibroblasts. *Oncogene* **19,** 3330–3334 (2000).
19. Nikiforov, M. A. *et al.* Complementation of Myc-dependent cell proliferation by cDNA expression library screening. *Oncogene* **19,** 4828–4831 (2000).
20. Lora, J. *et al.* Antisense glutaminase inhibition decreases glutathione antioxidant capacity and increases apoptosis in Ehrlich ascitic tumour cells. *Eur. J. Biochem.* **271,** 4298–4306 (2004).
21. Matsuno, T., Satoh, T. & Suzuki, H. Prominent glutamine oxidation activity in mitochondria of avian transplantable hepatoma induced by MC-29 virus. *J. Cell. Physiol.* **128,** 397–401 (1986).
22. Porkka, K. P. *et al.* MicroRNA expression profiling in prostate cancer. *Cancer Res.* **67,** 6130–6135 (2007).
23. Landgraf, P. *et al.* A mammalian microRNA expression atlas based on small RNA library sequencing. *Cell* **129,** 1401–1414 (2007).
24. Bode, B. P. Recent molecular advances in mammalian glutamine transport. *J. Nutr.* **131,** 2475S–2485S (2001).
25. Lobo, C. *et al.* Inhibition of glutaminase expression by antisense mRNA decreases growth and tumourigenicity of tumour cells. *Biochem. J.* **348,** 257–261 (2000).
26. Rabilloud, T. *et al.* The mitochondrial antioxidant defence system and its response to oxidative stress. *Proteomics* **1,** 1105–1110 (2001).
27. Anderson, T. J. *et al.* Discovering robust protein biomarkers for disease from relative expression reversals in 2-D DIGE data. *Proteomics* **7,** 1197–1207 (2007).
28. Kersey, P. J. *et al.* The International Protein Index: an integrated database for proteomics experiments. *Proteomics* **4,** 1985–1988 (2004).
29. Yates, J. R. III, Eng, J. K., McCormack, A. L. & Schieltz, D. Method to correlate tandem mass spectra of modified peptides to amino acid sequences in the protein database. *Anal. Chem.* **67,** 1426–1436 (1995).
30. Gao, P. *et al.* HIF-dependent antitumorigenic effect of antioxidants *in vivo*. *Cancer Cell* **12,** 230–238 (2007).

Supplementary Information is linked to the online version of the paper at www.nature.com/nature.

Acknowledgements The authors want to thank L. Blosser and A. Tam for their help in flow cytometry analysis, and H. Y. Zhang for her help with statistical analysis. This work was partially supported by NIH Awards NHLBI NO1-HV-28180, NCI R01CA051497, NCI R01CA57341, NCI R01CA120185, NCI P50CA58236, Rita Allen Foundation, Leukemia and Lymphoma Society, and Sol Goldman Center for Pancreatic Cancer Research.

Author Contributions P.G., K.K., T.O., A.M.D., J.E.V., J.T.M. and C.V.D. designed experiments. P.G., I.T., T.-C.C., Y.-S.L. and K.I.Z. performed experiments. K.K. and T.O. provided reagents. P.G. and C.V.D. wrote the paper. All authors discussed the results and commented on the manuscript.

Author Information Reprints and permissions information is available at www.nature.com/reprints. Correspondence and requests for materials should be addressed to C.V.D. (cvdang@jhmi.edu) or P.G. (pgao2@jhmi.edu).

METHODS

Cell culture. P493-6 human B lymphoma cells, PC3 human prostate cancer cells, CB33 lymphoblastoid cells, CB33-Myc cells and MCF7 human breast cancer cells were maintained in RPMI 1640 with 10% fetal bovine serum (FBS) and 1% penicillin-streptomycin. HT-29 cells were maintained in McCoy's 5A medium with 10% FBS and 1% penicillin-streptomycin. PC3-GLS1 and control PC3-GFP cells were established by infecting PC3 cells with retroviral supernatants from PQCXIN-GLS1 or PQCXIN-GFP vector-transfected phoenix cells. The cells were selected by and maintained with RPMI 1640 medium containing 500 μg ml^{-1} G418. Experiments under deprived glutamine or glucose culture conditions were performed by using RPMI 1640 without L-glutamine (GIBCO 21870) or RPMI 1640 without D-glucose (GIBCO 11879).

Mitochondrial protein enrichment. To enrich for mitochondrial protein, we adapted protocols as described[26]. 1×10^9 cells were used for high Myc (no tetracycline treatment) and 1.5×10^9 for tetracycline treated cells. Cells were harvested, washed with cold PBS extensively then washed with cold homogenization buffer (220 mM mannitol, 70 mM sucrose, 2 mM HEPES, pH 7.4 with KOH) to remove PBS. Harvested cell pellets were re-suspended in 8 ml of homogenization buffer with protease inhibitors (Roche), phosphatase inhibitors (EMD Chemicals) and homogenized with 15 strokes by a tight fitting dounce homogenizer. Homogenate was diluted with 60 ml of cold homogenization buffer and centrifuged at 800*g* for 10 min at 4 °C. The supernatant was collected and centrifuged at 7,000*g* for 15 min. The resulting pellet was homogenized in 8 ml homogenization buffer, diluted in 60 ml of the same buffer and centrifuged at 800*g* for 10 min. Supernatant was further centrifuged at 12,000*g* for 15 min. The mitochondrial pellet after this step was washed once more by re-suspending in 60 ml homogenization buffer and centrifugation for 15 min at 12,000*g*. Finally, the pellet was re-suspended in 1.5 ml of homogenization buffer, transferred to microcentrifuge tube, centrifuged at 16,000*g* for 20 min and solubilized in 40 μl of 5% ASB-14 (w/v) and then diluted in an appropriate amount of IEF buffer (8 M urea, 2 M thiourea, 4% w/v CHAPS, 1% w/v dithiothreitol, 0.5% v/v carrier ampholytes pH 4–7, and a trace amount of bromophenol blue) to make 5 mg ml^{-1} protein solution.

Two-dimensional gel electrophoresis and proteomics. Two-dimensional gel electrophoresis and mass spectrometry identification of proteins were performed as described with modifications[27]. A vMALDI linear ion trap mass spectrometer (vMALDI-LTQ, ThermoElectron) with XCalibur 1.4 SR1 software package was used to perform protein identification. Protein digests were re-suspended in 50% AcCN/0.1% TFA and mixed with an equal volume of 2,5-dihydroxybenzoic acid (2,5-DHB; Laser BioLab) 50 mg ml^{-1} in 50% acetonitrile/0.1% TFA. 0.5 μl of this mixture was spotted on a vMALDI plate. A survey scan from *m*/*z* 750 to *m*/*z* 4,000 (full MS) was followed by data-dependent MS/MS scans on 30 most intense ions with normalized collision energy value of 40, activation Q value of 0.25, and activation time of 30 ms. Raw data files were searched with BioworkBrowser 3.3 (ThermoElectron) against the IPI human protein sequence database, using search algorithm SEQUEST[28,29].

RNAi experiments. siRNAs targeting human *GLS1* (ON-TARGETplus SMARTpool, L-004548-01, target sequences are CCUGAAGCAGUUCGAAAUA, CUGAAUAUGUGCAUCGAUA, AGAAAGUGGAGAUCGAAAU and GCACAGACAUGGUUGGUAU), *MYC* (siGENOME SMART pool, J-003282-23, target sequences are ACGGAACUCUUGUGCGUAAUU, GAACACACAACGUCUUGGAUU, AACGUUAGCUUCACCAACAUU and CGAUGUUGUUUCUGUGGAAUU), or control siRNA (SiControl, D-001210-02, sequence is UAAGGCUAUGAAGAGAUAC) were purchased from Dharmacon Research Inc. Transfection of the siRNAs into P493 or PC3 cells was performed as described previously[30].

Knocking-down miR-23a/b with anti-sense LNA oligomers. miRCURY LNA knockdown probes for miR-23a (miRCURY knockdown, 118119-00, target sequence is AUCACAUUGCCAGGGAUUUCC) and miR-23b (miRCURY knockdown, 138120-00, target sequence is AUCACAUUGCCAGGGAUUACC), and for scramble miRNA (miRCURY knockdown, 199002-04, scramble-miR) LNA probes as negative control, were purchased from EXIQON, Inc. The transfection of LNA probes into cells was performed using the same protocol for siRNA transfection as described above.

3′ UTR luciferase assays and site-directed mutagenesis. The 3′ UTR sequence of human *GLS* was generated by PCR with the following primers: 5′-GCTCTAGACATGTGTATTTCTATCTGGTAGTG-3′ and 5′-GCTCTAGAGCATATCAGCAGATCATCACCATA-3′. The PCR products were digested with Xbal and then inserted into the PGL3 reporter vector downstream of the luciferase gene. The correct clones were confirmed by sequencing analysis. The mutagenesis of predicted miR-23a/b binding sites (seed sequences) was performed using a QuikChange site-directed mutagenesis kit (Stratagene, catalogue number 200519-5) and the following primers: 5′-CAATCTCCCTCCATGACGAGAGCAATATTACCTCG-3′ and 5′-GTTAGAGGGAGGTACTGCTCTCGTTATAATGGAGC-3′. For luciferase assay, cells were seeded in 48-well plates. After overnight incubation, cells were co-transfected either with 100 ng reporter vectors and 4 ng pSV-Renilla, or further co-transfected with 10 nM LNA antisense for miR-23a/b or control LNA. After 24 h, luciferase activities were measured using the Dual-Luciferase Reporter Assay System (Promega).

Chromatin immunoprecipitation and real-time PCR. Chromatin immunoprecipitation assay was carried out as described[7]. Chromatin immunoprecipitation primers for *C9orf3* were: amplicon A 5′-ATTCTTCTCTTGGCTGTTCTTTCC-3′, 5′-GAAGCAGCCAACTCTGTGGAG-3′; amplicon B 5′-GGAATACTAGGGTACCAGGGCA-3′, 5′-GCAGCTTGGCTGGCTAGG-3′; amplicon C 5′-ACTTAGGATCCAATCCACTGTTGAG-3′, 5′-CTCAACAGTGGATTGGATCCTAAGT-3′.

For real-time PCR, total RNA was extracted using the RNeasy kit (QIAGEN) followed by DNAase (Ambion) treatment according to the manufacturer's instructions. Primers were designed using Beacon Designer software, and cDNA was prepared using TaqMan Reverse Transcription Reagents (Roche, Applied Biosystems). The primers used were: GLS1-F, 5′-TGGTGGCCTCAGGTGAAAAT-3′; GLS1-R, 5′-CCAAGCTAGGTAACAGACCCTGTTT-3′; GLS2-F, 5′-AACGAATCCCTATCCACAAGTTCA-3′; GLS2-R, 5′-GCAGTCCAGTGGCCTTTAGTG-3′; 18s-F, 5′-CGGCGACGACCCATTCGAAC-3′; 18s-R, 5′-GAATCGAACCCTGATTCCCCGTC-3′. Quantitative real-time PCR for GLS1, GLS2 and 18S was performed using the ABI 7500 sequence detection system. All PCRs were performed in triplicate.

Immunoblot analysis. Rabbit antibody for GLS for immunoblots was described previously[10]. Rabbit anti-TFAM antibody was a gift from D. Kang. We used monoclonal anti-c-Myc antibody from Santa Cruz (9E10), and mouse antibody for tubulin from CalBiochem (CP06), and performed immunoblot assays according to the manufacturer's instructions.

Northern blot analysis. Northern blotting for miR-23a and miR-23b was performed as described[7] using Ultrahyb-Oligo (Ambion) and oligonucleotide probes perfectly complementary to the mature miRNA sequences.

Intracellular ATP. ATP levels were measured using a Somatic Cell ATP assay kit (Sigma) according to the manufacturer's instructions. Luminescence was measured using a Wallace microplate luminescence reader (Perkin Elmer) and normalized to the protein concentration.

Flow cytometric measurement of glutathione, ROS and cell death. The measurement of glutathione levels in cells was performed using monobromobimane (Sigma Aldrich) as described previously[19]. Intracellular ROS production was measured by staining cells with dichlorodihydrofluorescein diacetate (Molecular Probes). Cell apoptosis was detected using an Annexin V-PE Apoptosis Detection Kit (BD Pharmingen, catalogue number 559763). Stained cells were analysed in FACScan flow cytometers (BD Bioscience).

Measurement of cellular O_2 consumption. Cells were harvested and re-suspended at 1×10^7 per ml in RPMI1640 medium with 10% FBS and 25 mM HEPES buffer. For each experiment, equal numbers of cells suspended in 0.5 ml were pipetted into the chamber of an Oxytherm electrode unit (Hansatech Instrument Ltd), which uses a Clark-type electrode to monitor the dissolved oxygen concentration in the sealed chamber over time. The data were exported to a computerized chart recorder (Oxygraph, Hansatech Instrument Ltd), which calculated the rate of O_2 consumption. The temperature was maintained at 37 °C during the measurement. The O_2 concentration in 0.5 ml of RPMI1640 medium without cells was also measured over time to provide background values. Relative O_2 consumption rate was calculated after correcting for background.

TaqMan microRNA assays. We purchased TaqMan microRNA assay kits for hsa-miR-23a (catalogue number 4373074) and has-miR-23b (catalogue number 4373073) and control probes from Applied Biosystems, and performed real-time PCR assays according to the manufacturer's instructions.

Human prostate cancer samples. Human samples were acquired with the approval of the Johns Hopkins University School of Medicine Institutional Review Board.